# Linear and non-linear modelling of dynamic behaviour of cracked reinforced concrete beams

Z. Huszár
*Department of Reinforced Concrete Structures, Technical University of Budapest, H-1111 Budapest, Hungary*
*EMail: zshuszar@epito.bme.hu*

## Abstract

The dynamic behaviour of bent reinforced concrete beams in elastic range is significantly influenced by cracks caused by former loads. Considering this fact a more accurate calculation of the eigenfrequencies of the beams subjected to dynamic effects is available.

Experiments have shown that the features of vibration differ from the results obtained by the well-known linear model, if cracked zones exist. The cause of this phenomenon is that the bending rigidity of the cross-sections in the cracked range depends on the sign of the actual bending moment. The flexural stiffness of the cracked reinforced concrete beam, in bending vibration, changes periodically. Therefore the vibration shows non-linear characteristics in the elastic range as well. The cracked zone causes geometric non-linearity.

For a detailed investigation of the problem, experiments and linear and non-linear analysis were performed.

## 1 Introduction

The dynamic behaviour of the cracked reinforced concrete beam was examined by experiments in the Laboratory of Reinforced Concrete Structures at the Technical University of Budapest [1].

First, in that experiment in the middle third part of the examined reinforced concrete beam cracks were induced by so large $P$ forces, where the bending moment exceeded the cracking moment (Fig. 1).

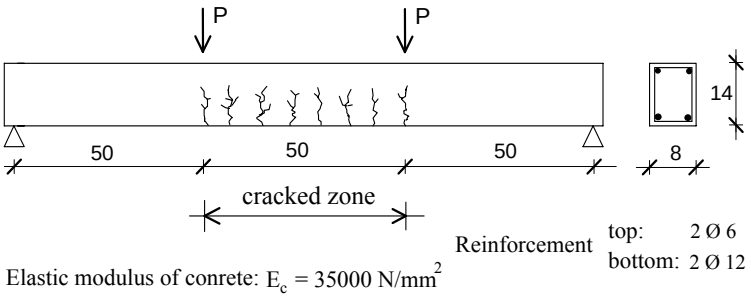


Figure 1. Model used at the experiments

After removing the static *P* forces, the beam was brought into vibration with an exterior impact load, by a rubber hammer blow. According to the spectral decomposition of the time-deflection series (Fig. 2), the first eigenfrequency resulted in 98 Hz. In addition a secondary peak has also appeared at 89 Hz.

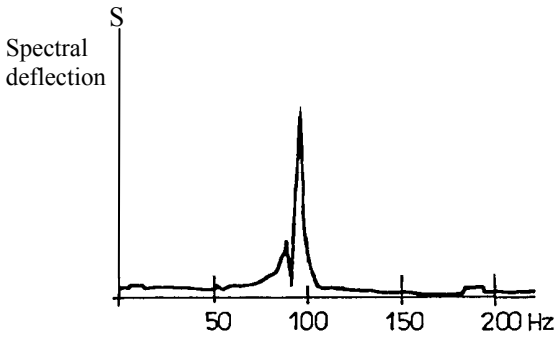


Figure 2. Time-deflection spectrum obtained in the experiment

If the beam will be considered free from cracks, then the eigenfrequencies can be determined in an elementary way with the well-known formula (1) [2]:

$$f_n = \frac{\pi}{2}\left(\frac{n}{\ell}\right)^2 \sqrt{\frac{EI}{m}} \qquad (1)$$

The first three eigenfrequencies of the uncracked beam are displayed in Table 1.

Table 1.

| | $f_1$ [Hz] | $f_2$ [Hz] | $f_3$ [Hz] |
|---|---|---|---|
| Elementary calculation | 109 | 436 | 981 |

According to expectations, the first eigenfrequency of the uncracked beam is larger than the result shown in the experiment. The cause of this difference is that during the vibration the bending rigidity of the cross-sections in the cracked range is not constant. It depends, whether cracks close or open. If cracks were caused by positive moments, the flexural stiffness of the beam in the cracked zones can be described with the formula below:

$$EI_i = \begin{cases} E_c I_{i,I} & \text{if} \quad M_i < 0 \\ E_c I_{i,II} & \text{if} \quad M_i \geq 0 \end{cases} \tag{2}$$

where: $I_{i,I}$ is the moment of inertia of the uncracked section and $I_{i,II}$ is that of the cracked section.

So the vibration shows non-linear characteristics in the elastic range as well. In this case only virtual eigenfrequencies could be investigated.

## 2 The computation method

The dynamic behaviour of the cracked beam in the elastic range, can be described by the well-known differential equation with varying coefficients [2]:

$$\frac{\partial^2}{\partial x^2}\left( EI(x)\frac{\partial^2 w}{\partial x^2} + c_s I(x)\frac{\partial^3 w}{\partial x^2 \partial t} \right) + c\frac{\partial w}{\partial t} + m(x)\frac{\partial^2 w}{\partial t^2} = q(x,t) \tag{3}$$

where: $x$ is the coordinate in axial direction, $w(x,t)$ is the displacement perpendicular to the axis of the beam, $EI(x)$ is the flexural stiffness, $c_s$ and $c$ are the damping coefficients, $m(x)$ is the specific mass per unit length and $q(x,t)$ is the external distributed load.

The solution of the non-linear vibration problem needs discretising in time and in space. The discretising in the axial direction was made with the difference method. The beam model (Fig. 1) was in the calculation divided in 18 equal parts along the longitudinal axis. For the description of the relationship between the bending moment and the deflection eqn (4), as well as of the relationship between the loading and the bending moment eqn (5), the difference operators were used:

$$M_i = -EI\frac{\partial^2 w}{\partial x^2} \approx -\frac{EI}{\Delta\ell^2}(w_{i-1} - 2w_i + w_{i+1}) \tag{4}$$

$$q_i = -\frac{\partial^2 M}{\partial x^2} \approx -\frac{1}{\Delta\ell^2}(M_{i-1} - 2M_i + M_{i+1}) \tag{5}$$

where: $\Delta\ell$ is the distance of the dividing points.

Making use of eqns (3), (4), (5), the equation of motion for the discrete system, eqn (6) can be assembled. In the equation below the $\{u\}$ vector contains the $w_i$ vertical displacements of the nodal points.

$$[K]\{u\} + [C]\{\dot{u}\} + [M]\{\ddot{u}\} = \{F(t)\} \tag{6}$$

With the difference operators the $[K]$ stiffness-, $[C]$ damping- and $[M]$ mass matrices can be composed. In this computation the Rayleigh damping was applied. The damping matrix was assembled as a linear combination of the stiffness- and mass matrix:

$$[C] = a[K] + b[M] \tag{7}$$

The application of the Rayleigh damping results in uncoupled mode shapes, similarly to the undamped case [2].

The equation of the motion (6) contains already the boundary conditions, the hinged supports at both ends of the beam. In the case of constant flexural stiffness in time, the modal solution of the vibration problem can be obtained by eqn (6).

Considering the non-linear properties, due to the relation (2), makes it necessary the discretising in time, by applying a time-step algorithm. For that purpose the method of central differences was used. To insure convergence and adequate accuracy, the time-step must be considerably shorter than the smallest vibration period in the model [3]. The applied algorithm is based on constant acceleration within the time-steps.

On basis of the above method a MATLAB program was elaborated.

## 3 Numerical investigations

With the MATLAB program there were numerical simulations carried out on the linear and non-linear computing model of the beam in Fig. 1. For the sake of a detailed analysis of the dynamic behaviour of the beam the non-linear analysis was performed both with and without considering the gravitational forces.

### 3.1 Examinations on the linear model

The linear vibration problem can be solved assuming a constant flexural stiffness in time. This makes possible the estimation of the virtual eigenfrequencies of the

beam in Fig. 1, by giving upper and lower boundaries. A lower boundary can be obtained, if in the cracked region the smaller flexural stiffness $EI_{II}$ is substituted and regarded as constant in time. This would be the model of a beam in which cracks are produced in the middle third region at both faces by positive and negative moments (weakened beam). To obtain the upper boundary for the investigated eigenfrequencies, the greater flexural stiffness $EI_I$ should be applied in the middle part. With this constant $EI_I$ an uncracked beam is modelled.

In the undamped case, the eigenfrequencies can be derived, by solving the eigenvalue problem, coming from eqn (6):

$$([K]-\omega_i^2\,[M])\{u_i\} = 0 \tag{8}$$

With making use of the computing model the first three eigenfrequencies of the uncracked beam and of the weakened beam was determined. The results are shown in Table 2. It can be seen that the first virtual eigenfrequency obtained in the experiment is surrounded by the results of the linear calculations: the beam without crack (upper boundary) and the weakened beam (lower boundary).

Table 2.

| | $f_1$ [Hz] | $f_2$ [Hz] | $f_3$ [Hz] |
|---|---|---|---|
| Linear computation, uncracked beam | 109 | 436 | 981 |
| Experiment, real beam | 98 | | |
| Linear computation, weakened beam | 85 | 397 | 862 |

### 3.2 Examinations on the non-linear model, neglecting the gravitational forces

Considering the periodically varying flexural stiffness in time (2), on the non-linear model a free vibration problem was examined. For this purpose an impact load was modelled in the section $x=\ell/3$, as follows:

$$F(t,x) = \begin{cases} F_0 & \text{if} \quad t \le \Delta t \quad \text{and} \quad x = \ell/3 \\ 0 & \text{if} \quad t > \Delta t \end{cases} \tag{9}$$

This corresponds essentially to the experiment carried out on the beam presented in Fig. 1. In order to establish stability in the explicit method, the $\Delta t$ time-step was chosen as very small [3], that is 1/1000 of the first eigenperiod of the uncracked beam. The power acting in $\Delta t$ corresponds to one Dirac impulse. The Dirac unit pulse is representing a square-wave with a length of time tending to zero, while it's definite integral equals 1 unit. A 1 sec time-interval of the vibration was examined, into which 109000 time-steps fell. In Fig. 3 the time-deflection diagram is given at the cross-section $x=\ell/3$, between time-steps 1-4000.

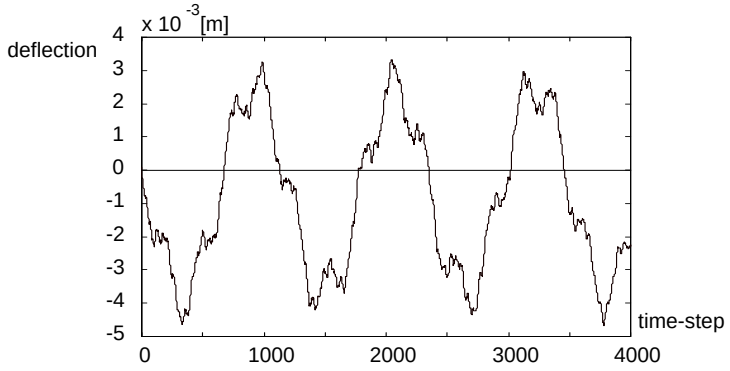


Figure 3. Time-deflection diagram immediately after the load impulse

Fig. 3 demonstrates properly that the Dirac impulse induces all eigenfrequencies (white noise [2], [4]).

The virtual eigenfrequencies of this quasi-periodical motion was determined by discrete Fourier transformation [5] of the time-deflection data series. On Fig. 4 it can be seen that the spectrum range 0-500 Hz contains the first two eigenfrequencies. The third eigenfrequency did not appear, because mode shape 3 has a nodal point in the cross-section of the impact load action. The first virtual eigenfrequency according to Fig. 4 was 96 Hz. It means that the non-linear calculation and the experiment have shown a good coincidence.

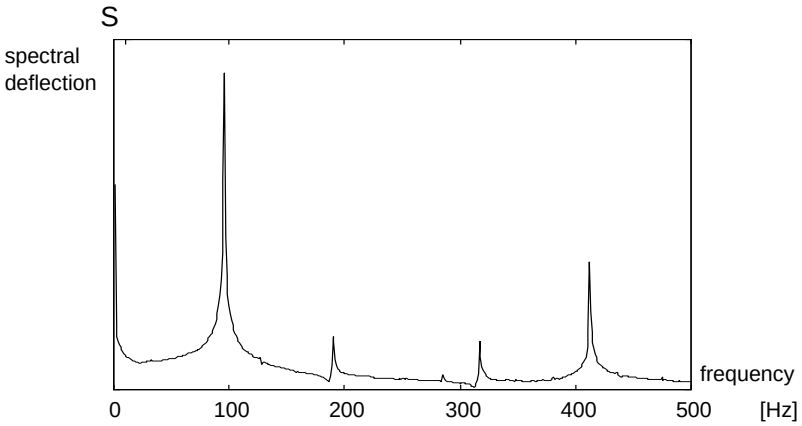


Figure 4. The spectral decomposition of the time-deflection

### 3.3 Examinations on the non-linear model considering the gravitational forces

The computation model in Chapter 3.2 does not show the spontaneous separation of the first eigenfrequency, namely the existence of the secondary peak in Fig. 2. To the first eigenmode belongs only one virtual eigenfrequency (Fig. 4).

However, when taking into consideration the self-weight, the situation changes. Due to the self-weight cracks open in the middle region, already in the static condition. Thus the stepwise change of the flexural stiffness is the following:

$$EI_i = \begin{cases} E_c I_{i,I} & \text{if} \quad M_{dyn,i} + M_{stat,i} < 0 \\ E_c I_{i,II} & \text{if} \quad M_{dyn,i} + M_{stat,i} \geq 0 \end{cases} \tag{10}$$

This means a shifting of the base line compared with relation (2). In case of a sufficiently large starting impulse, in the first part of the observed vibration the cracks still close in each period when negative resultant moment arises. In the second part of the time-interval as dynamic moment becomes smaller due to damping, the cracks will not close. The double peak can appear in the spectrum if there is an appropriate relation among the starting impulse, the self-weight and the damping.

Taking the self-weight into assumption, the vibration spectrum was produced by the Wilson type time-step integral, which is shown in Fig. 5. In this calculation Rayleigh damping was applied. The linear combination (7) had been chosen so that it showed in case of the uncracked beam in the first mode 1.5% and in the third mode 10% damping. That means a damping between 1.5-2%, near the first virtual eigenfequency of the cracked beam.

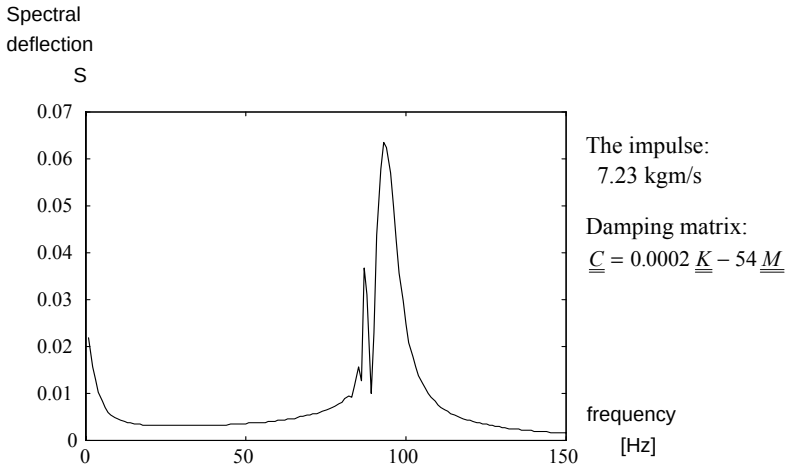


Figure 5. Double peak in the spectrum of the beam model

The first virtual eigenfrequencies, according to the spectrum, have the values in 87 Hz and 94 Hz. In the experiment these frequencies have been found to be 89 Hz, and 98 Hz.

The main peak (94 Hz) derived from this non-linear analysis with self-weight is a little smaller than the 96 Hz, obtained from the previous non-linear calculation without self-weight. That is because of the self-weight, the smaller flexural stiffness of the cracked section is valid for a little longer segment of the periods than before. The secondary peak represents a larger frequency than the lower boundary 85 Hz, obtained from the linear calculation of the weakened beam. It is worth mentioning that the double peak here does not mean two frequencies of a quasi-resonant state. The essence of the phenomenon is that the examined interval of the vibration is divided into two parts. In the first part the cracks still close, but in the second part they do not. This is due to the decreasing vibration amplitude. In case of forced harmonic vibration of continuously increasing frequency, only one quasi-resonant state can be found in the first mode.

The results of the non-linear examinations are summed up in Table 3.

Table 3.

| | $f_1$ [Hz] | $f_2$ [Hz] |
|---|---|---|
| Non-linear computation, without self-weight | 96 | 414 |
| Non-linear computation, with self-weight | 87, 94 | |

In general cases, when considering different ratios of static loads (containing the self-weight) and dynamic loads, the virtual eigenfrequency falls in an interval determined by two extreme cases:

1. When large self-weight or static forces are coupled with small dynamic loads, the vibration of the beam is similar to the behaviour of the weakened beam in chapter 3.1.
2. When the static loads are relatively small compared with the dynamic loads, the vibration of the beam is similar to the case shown in chapter 3.2.

## 4. Approximation of the first two virtual eigenfrequencies

The first two virtual eigenfrequencies of the non-linear vibration can also be found by combination of simple linear models, when neglecting the gravitational forces.

### 4.1 Approximation of the first virtual eigenfrequency, with a single-degree-of-freedom model

The approximate value of the first eigenfrequency can be obtained, from non-linear vibration of the single-degree-of-freedom (SDOF) system (Fig. 6).

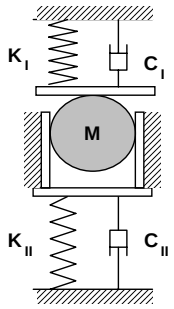


Figure 6. SDOF Model

In the vibrating system (Fig. 6) the $M$, $K_I$, $C_I$ elements represent the closing of the cracks, while the $M$, $K_{II}$, $C_{II}$, elements represent the opening. Therefore, one period of the examined vibration consists of two different pieces of half sine-waves with different periods and different amplitudes. The length of the period of this (quasi periodic) motion is given by the sum of the two different half-periods. Consequently the virtual eigenfrequency $f_1^*$, can be calculated from the relation (11), which resulted in 95.8 Hz:

$$f_1^* = \frac{1}{\frac{1}{2f_1^I} + \frac{1}{2f_1^{II}}} \tag{11}$$

where: $f_1^I$ is the first eigenfrequency of the uncracked beam, $f_1^{II}$ represents the eigenfrequency of the weakened beam, found by linear calculation with flexural stiffness $EI_{II}$ in the cracked zone.

To the calculation of $f_1^I$ the well-known closed formula is available. To compute the $f_1^{II}$ the modal analysis on the discrete system is applicable.

The formula (11) approaches the first virtual eigenfrequency of the beam represented in Fig. 1, fairly well.

### 4.2 Approximation of the second virtual eigenfrequency, with linear models

The second virtual eigenfrequency of the cracked beam can be approximated also with simple linear models, applying the modal analysis.

The non-linear vibration of the beam in Fig. 1 is started with an initial velocity distribution of a full sine-wave, which is typical for the second mode of the uncracked beam. In Fig. 7 can be seen the different phases of the vibration.

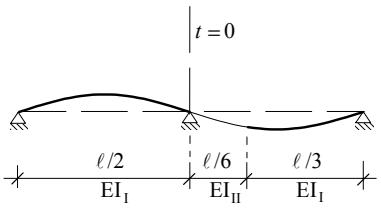


Figure 7.a Eigenmode and static system in time $t = 0$

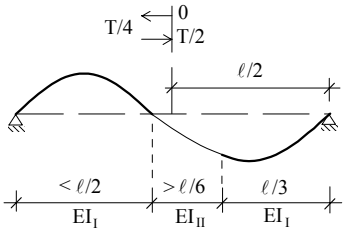


Figure 7.b
Eigenmode in the first half-period

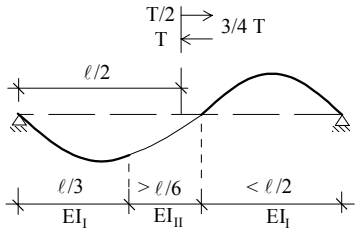


Figure 7.c
Eigenmode in the second half-period

When starting the vibration, in time *t=0* the inflexion point of the mode-shape is at the midspan (Fig. 7.a). Therefore it can be modelled with the vibration of a two-span beam with distances of $\ell/2$ between the supports.

In the first half-period (Fig. 7.b) in the cracked zone, on right of the inflexion point, the cracks open. The flexural stiffness therefore takes here the value $EI_{II}$. On the left of the inflexion point the cracks close, so the flexural stiffness remains still $EI_I$. Because of the asymmetry of the stiffness distribution, the inflexion point moves continuously to the left. Therefore the length of the region with flexural stiffness $EI_{II}$ slightly increases. The extreme position will be reached, after a quarter of period. In the second half-period (Fig. 7.c) the stiffness distribution is mirrored at the midspan. The length of the region with stiffness $EI_{II}$ varies in the same way, as in the first half-period.

In this sense the inflexion point is oscillating around the midspan according to the virtual eigenfrequency. So in the second mode of the non-linear vibration, during one period, the length of the section with flexural stiffness $EI_{II}$ is changing periodically. For the determination of the second virtual eigenfrequency, a better approximation of the upper and lower boundary can be given, with the combination of linear models, as in Table 2.

The model according to Fig. 7.a gives the upper boundary of the second virtual eigenfrequency. In the time $t=0$ the length of the region with the $EI_{II}$ bending rigidity is the smallest ($\ell/6$).

The configuration in Fig. 7.b at time $t=T/4$ supplies the lower boundary of the second virtual eigenfrequency. In that case the length of the zone with flexural stiffness $EI_{II}$ is the largest ($>\ell/6$).

A modal analysis on a finite-element model with a fine mesh has shown that the displacement of the inflexion point is small. It causes in the eigenfrequency a change less than 1%, which is 417.6 Hz in case Fig. 7.a and 417.4 Hz in case Fig. 7.b.

## 5 Comparison of the experiments and the calculations

The results of the experiments and the calculations are summarized in Table 4. The calculations of non-linear examinations and simplified linear models show good coincidence with the experiments. Table 4 shows that the combination of simplified linear models can be applied with good results, for analysing non-linear vibrations. The double peak, which appeared in the spectrum of experiments, can be obtained also by numerical simulation.

Table 4.

| | $f_1$ [Hz] | $f_2$ [Hz] |
|---|---|---|
| Experiment, real beam | 89, 98 | |
| Linear computation, uncracked beam | 109 | 436 |
| Linear computation, weakened beam | 85 | 397 |
| Non-linear computation, without self-weight | 96 | 414 |
| Non-linear computation, with self-weight | 87, 94 | |
| Approximate simplified models | 95.8 | 417.5 |

## References


1. Nguyen, V. C., *Experimental investigation of bending vibration of beams, (in Hungarian),* Ph.D. Theses Budapest, pp 20, pp 51, 1994.
2. Clough, R. W. & Penzien, J., *Dynamics of Structures,* Mc Graw-Hill Book Company, New York, 1975.
3. Bathe, K. J. & Wilson, E. L., *Numerical Methods in Finite Element Analysis,* Prentice Hall, Inc., Englewood Cliffs, N. J., 1976.
4. Pfaffinger D. D., *Tragwerksdynamik*, Springer Verlag, Wien, New York, 1988.
5. Korn, G. A. & Korn, T. M., *Mathematical Handbook for Engineers, (in Hungarian),* Műszaki Könyvkiadó Budapest, 1975.

6. Ulm, F .J. & Clement, J. L. & Afra, H. & Argoul, P., *Frequenzverlust und kritische Dämpfung im Bruchzustand. Stahlbetonkonstruktionen unter dynamischen Lasten,* Bauingenieur v.68, no.4, pp. 183-190, 1993.
7. Krauthammer, T. & Shahriar, S. & Shanaa, H. M., *Response of reinforced concrete elements to severe impulsive loads,* Journal of Structural Engineering v.116, no.4, pp. 1061-1079. 1990.
8. Jerath, S. & Shibani, M. M., *Dynamic stiffness and vibration of reinforced concrete beams,* Journal of the American Concrete Institute v.82, no.2, pp. 196-202. 1985.
9. Dieterle, R. & Bachmann, H., *Einfluss der Rissbildung auf die dynamischen Eigenschaften von Leichtbeton- und Betonbalken,* Schweizer Ingenieur und Architekt v.98, no.32, pp. 715-721. 1980.

# Linear and non-linear modelling of dynamic behaviour of cracked reinforced concrete beams

Z. Huszár

**Key words:**

Cracked beam,
dynamic behaviour,
geometric non-linearity,
virtual eigenfrequency,
Fourier transformation